Journal of Zhejiang University-SCIENCE B (Biomedicine & Biotechnology) 2022 23(3):230-240
www.jzus.zju.edu.cn; www.springer.com/journal/11585
E-mail: jzus_b@zju.edu.cn

Correspondence

https://doi.org/10.1631/jzus.B2100807

Check for updates

A new benzaldehyde from the coral-derived fungus *Aspergillus terreus* C23-3 and its anti-inflammatory effects via suppression of MAPK signaling pathway in RAW264.7 cells

Minqi CHEN[1,2*], Jinyue LIANG[1*], Yuan WANG[1], Yayue LIU[1,2,3,4], Chunxia ZHOU[1,2,3,4], Pengzhi HONG[1,2,3,4], Yi ZHANG[1,2,3,4✉], Zhong-Ji QIAN[1,2,3✉]

[1]*College of Food Science and Technology, School of Chemistry and Environment, Guangdong Ocean University, Zhanjiang 524088, China*
[2]*Shenzhen Institute of Guangdong Ocean University, Guangdong Ocean University, Shenzhen 518108, China*
[3]*Southern Marine Science and Engineering Guangdong Laboratory, Zhanjiang 524025, China*
[4]*Collaborative Innovation Center of Seafood Deep Processing, Dalian Polytechnic University, Dalian 116034, China*

Marine fungi are important members of the marine microbiome, which have been paid growing attention by scientists in recent years. The secondary metabolites of marine fungi have been reported to contain rich and diverse compounds with novel structures (Chen et al., 2019). *Aspergillus terreus*, the higher level marine fungus of the *Aspergillus* genus (family of Trichocomaceae, order of Eurotiales, class of Eurotiomycetes, phylum of Ascomycota), is widely distributed in both sea and land. In our previous study, the coral-derived *A. terreus* strain C23-3 exhibited potential in producing other biologically active (with antioxidant, acetylcholinesterase inhibition, and anti-inflammatory activity) compounds like arylbutyrolactones, territrems, and isoflavones, and high sensitivity to the chemical regulation of secondary metabolism (Yang et al., 2019, 2020; Nie et al., 2020; Ma et al., 2021). Moreover, we have isolated two different benzaldehydes, including a benzaldehyde with a novel structure, from *A. terreus* C23-3 which was derived from *Pectinia paeonia* of Xuwen, Zhanjiang City, Guangdong Province, China.

Benzaldehydes are frequently reported natural products from *Aspergillus* spp., *Chaetomium* sp., *Eutotium* sp., and the like. In a benzaldehyde, the carbon-oxygen double bond on the aldehyde group is conjugated with the large π bond on the benzene ring, having a total of 8 π electrons. These types of compounds usually display remarkable bioactivity like antimicrobial, anti-inflammatory, antitumor, cytotoxic, and antioxidant effects (Umeda et al., 1974; Wang et al., 2006; Kim et al., 2014; Machado et al., 2021).

Inflammation, a self-regulated reaction process of the human body to infection, external stimulation, or injury, is the manifestation of a stress state that is beneficial to the human body in moderation. Yet, excessive inflammation will lead to tissue damage and induce inflammatory-related diseases (Xin et al., 2020). Many studies have found that nuclear factor-κB (NF-κB) is a central transcriptional factor that can regulate inflammatory factors such as interleukin (IL)-6, nitric oxide (NO), and cyclooxygenase-2 (COX-2) (Hayden and Ghosh, 2008; Pinho-Ribeiro et al., 2016; Afonina et al., 2017; Zucoloto et al., 2017). Among these mediators, NO produced by inducible nitric oxide synthase (iNOS), due to its properties as a free radical, might cause some unwanted and negative effects (Lawrence et al., 2002; Li et al., 2014; Yamanishi et al., 2014). Excessive NO production might give rise to inflammatory diseases, such as headaches, dizziness, low blood pressure, and rheumatoid arthritis (Moncada and Higgs, 1991). iNOS, as one of three key enzymes generating NO from the amino acid L-arginine, can mediate host defense mechanisms and

✉ Yi ZHANG, hubeizhangyi@163.com
Zhong-Ji QIAN, zjqian78@163.com
* The two authors contributed equally to this work
Yi ZHANG, https://orcid.org/0000-0002-1600-7456
Zhong-Ji QIAN, https://orcid.org/0000-0001-9220-2600

Received Sept. 17, 2021; Revision accepted Dec. 15, 2021; Crosschecked Feb. 15, 2022

obliterate bacterial, viral, fungal, and parasitic infections (Marletta, 1993; Kröncke et al., 1998; Aktan, 2004).

In addition, the metabolism of oxygen can impact inflammation response. There is a large body of evidence that reactive oxygen species (ROS) may be critical in the molecular mechanism of a range of inflammatory-associated diseases (Martínez-Soto and Ruiz-Herrera, 2017). Besides, the mitogen-activated protein kinase (MAPK) pathway in all of the eukaryotic organisms (including animals, plants, and fungi) is one of the most significant and conserved evolutionary mechanisms for sensing extracellular information (Martínez-Soto and Ruiz-Herrera, 2017). MAPKs, which include c-Jun N-terminal kinase (JNK), extracellular signal-related kinase (ERK)-1/2, and p38, are the typical inflammation-related signals (Li et al., 2018).

In this study, two benzaldehyde derivatives (**1** undescribed and **2** known; Fig. 1) were characterized from their fermentation products. We reported their isolation, structural elucidation, and anti-inflammatory effects on lipopolysaccharide (LPS)-induced macrophage cells.

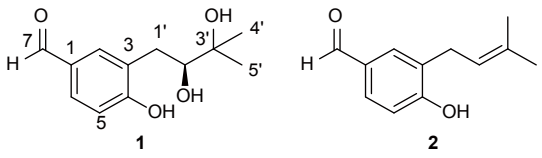

Fig. 1 Structures of compounds 1 and 2.

The two benzaldehydes (**1** and **2**) were obtained by repeated column chromatography on silica gel and subsequent preparative high-performance liquid chromatography (HPLC) from the static fermentation of the producer strain.

Compound **1**, with the appearance of yellowish glue with melting point (m.p.) of 113.2–115.3 ℃, showed a typical 1,3,4-trisubstituted benzene ring with proton signals in ^{1}H-nuclear magnetic resonance (NMR) spectrum (Table 1), including ^{1}H-NMR chemical shift δ_H (ppm, 1 ppm=1×10^{-6}) 7.67 (^{1}H, d, J=2.0 Hz, H-2), 6.89 (^{1}H, d, J=8.3 Hz, H-5), and 7.66 (^{1}H, dd, J=8.4, 2.0 Hz, H-6). The signals of a formyl group (δ_H 9.78 (^{1}H, s, H-7), ^{13}C-NMR chemical shift δ_C (ppm) 192.99 (C-7)) showed heteronuclear multiple bond correlations (HMBCs) (Fig. 2) with the benzene ring, including HMBCs from H-7 to C-1 (δ_C 130.98) and C-2 (δ_C 134.01), from H-2 to C-1 and C-7, from H-6 to C-7, and from H-5 to C-1, allocating this group to C-1. The ^{1}H-^{1}H correlation spectroscopy (COSY) between methylene protons (δ_H 3.11 (^{1}H, dd, J=16.7, 5.0 Hz, H_a-1') and 2.81 (^{1}H, dd, J=16.7, 6.9 Hz, H_b-1')) and an oxygenated methine proton (δ_H 3.82 (^{1}H, dd, J=6.9, 5.1 Hz, H-2')) and the HMBC correlations from H-1' to C-2' (δ_C 69.70) and an oxygenated quaternary carbon (δ_C 79.90 (C-3')) and from H-2' to two methyl carbons (δ_C 21.73 (C-4') and 25.86 (C-5')) suggested the presence of a 2,3-dihydroxy-3-methyl-butyl side chain. Moreover, the HMBC correlations from H_a-1'/H_b-1' to C-2 and two quaternary carbons (δ_C 122.02 (C-3) and 160.50 (C-4)) linked the C_5-side chain to C-3. The ortho-effect of oxygenation, as shown by the up-field chemical shifts of H-5 and C-5 (δ_C 118.75) and the HMBC correlations from H-2, H-5, H-6 and H_a-1'/H_b-1' to

Table 1 NMR data of compounds 1 and 2 using TMS as internal standard

Position	Compound **1**		Compound **2**	
	δ_C	δ_H	δ_C	δ_H
1	130.98		131.54	
2	134.01	7.67 (^{1}H, d, J=3.0 Hz)	129.94	7.61 (^{1}H, d, J=2.0 Hz)
3	122.02		130.50	
4	160.50		163.55	
5	118.75	6.89 (^{1}H, d, J=8.3 Hz)	116.08	6.87 (^{1}H, d, J=8.2 Hz)
6	130.43	7.66 (^{1}H, dd, J=8.4, 2.0 Hz)	134.01	7.59 (^{1}H, dd, J=8.2, 2.1 Hz)
7	192.99	9.78 (^{1}H, s)	193.12	9.70 (^{1}H, s)
1'	31.83	3.11 (^{1}H, dd, J=16.7, 5.0 Hz) 2.81 (^{1}H, dd, J=16.7, 6.9 Hz)	28.94	3.32 (^{2}H, d, J=7.4 Hz)
2'	69.70	3.82 (^{1}H, dd, J=6.9, 5.1 Hz)	122.94	5.32 (^{1}H, m)
3'	79.70		132.26	
4'	21.73	1.32 (^{3}H, s)	25.94	1.75 (^{3}H, s)
5'	25.86	1.36 (^{3}H, s)	17.82	1.71 (^{3}H, s)

700 MHz for ^{1}H-NMR and 175 MHz for ^{13}C-NMR. Solvent: CD_3OD. NMR: nuclear magnetic resonance; TMS: tetramethylsilane.

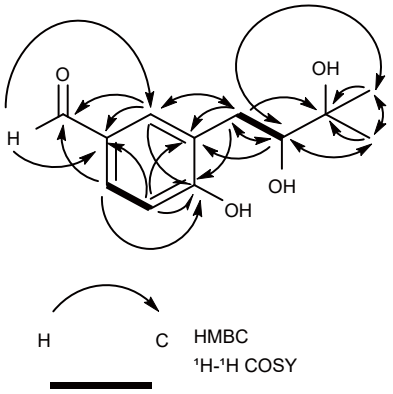

Fig. 2 Selected HMBC and ^{1}H-^{1}H COSY correlations of compound 1. HMBC: heteronuclear multiple bond correlation; COSY: correlation spectroscopy.

C-4, suggested that a hydroxy group is located at C-4. Thus, the compound was determined to have a planar structure, which was supported by the high-resolution mass spectrum presenting strong dehydrated ions at mass-to-charge ratio (*m*/*z*) 207.1017 $[M+H-H_2O]^+$ ($C_{12}H_{15}O_3^+$, calculated (calc.) 207.1016) and 229.0830 $[M+Na-H_2O]^+$ ($C_{12}H_{14}O_3Na^+$, calc. 229.0835) (Figs. S1–S7).

In order to determine the absolute configuration at C-2', the specific optical rotation of **1** was measured, resulting in the values of $[\alpha]_D^{25}$ –13.2 (*c*. 0.243, $CHCl_3$). When compared with the property of leptoic acid A with R configuration at C-2' ($[\alpha]_D^{25}$ +30.0 (*c*. 0.150, $CHCl_3$), a highly similar compound only with a difference at C-1 in its planar structure (a carboxyl group replaces thed formyl group in **1**) (Zhao et al., 2017), compound **1**, was determined to possess S configuration at C-2'. Hence, compound **1** was elucidated as an undescribed compound (*S*)-3-(2,3-dihydroxy-3-methylbutyl)-4-hydroxybenzaldehyde, and named as terreusol.

Compound **2** was elucidated as the known compound 4-hydroxy-3-(3-methylbut-2-en-1-yl)-benzaldehyde (Cho and Kim, 2012) by NMR data comparison with literature report (Table 1).

Cytotoxicity was determined by the 3-(4,5-dimethylthiazol-2-yl)-2,5-diphenyltetrazolium bromide (MTT) method. RAW264.7 cells were treated with the two benzaldehydes (**1** and **2**) in the doses of 0.1, 1.0, and 10.0 μmol/L, separately. The cellular viability of all dose groups was similar to the blank group, with no significant differences observed (Fig. 3a). Thus, the concentrations of 0.1, 1.0, and 10.0 μmol/L of the two benzaldehydes (**1** and **2**) could be used for the further experiment.

The production of NO by RAW264.7 cells was rationed and quantified by the Griess assay. The concentrations of NO in the groups treated with 0.1, 1.0, and 10.0 μmol/L of the two benzaldehydes were 10.72, 9.94, 9.42 μmol/L (**1**) and 12.87, 12.48, 11.78 μmol/L (**2**), respectively, as illustrated in Fig. 3b, and those of the blank group and control group were 9.00 and 14.78 μmol/L, respectively. Overall, it could be assumed that the concentration of NO in RAW264.7 was increased after cells were exposed to LPS (Fig. 3b), and this level was decreased in B-**1** (benzaldehyde **1**) and B-**2** (benzaldehyde **2**) groups in a dose-dependent fashion.

The above results reflected that both of the two benzaldehydes (**1** and **2**) in doses of 0.1, 1.0, and 10.0 μmol/L could markedly decrease the production of NO in RAW264.7 cells.

The RAW264.7 cells treated with the two benzaldehydes (**1** and **2**) and LPS were measured with 2,7-dichlorodihydrofluorescein diacetate (DCFH-DA) assay to determine the production of ROS. In this assay, the amount of ROS production was measured by fluorescence intensity. As shown in Figs. 4a and 4b, the amount of ROS production was 50.63% in the blank group and soared to 70.21% in the control group, while those in the groups treated with the two benzaldehydes in the doses of 0.1, 1.0, and 10.0 μmol/L were only 57.24%, 55.73%, 46.44% (**1**) and 54.43%, 48.33%, 46.89% (**2**), respectively, showing down-regulation with dose dependency.

According to the above results, the two benzaldehydes (**1** and **2**) could effectively reduce the ROS production in RAW264.7 cells. In addition, both the B-**1** and B-**2** groups revealed significant differences compared with the control group. The ROS production of the high-dose group (10.0 μmol/L) in the B-**1** and B-**2** groups was similar to that in the blank group, suggesting that both the two benzaldehydes (**1** and **2**) could effectively reduce ROS production in the cells.

RAW264.7 cells were treated with the two benzaldehydes (**1** and **2**) before the IL-6 levels were measured through enzyme-linked immunosorbent assay (ELISA). As shown in Fig. 4c, the production levels of IL-6 in stimulated cells increased significantly. On the contrary, the levels of IL-6 in the B-**1** and B-**2** groups decreased in a dose-dependent manner.

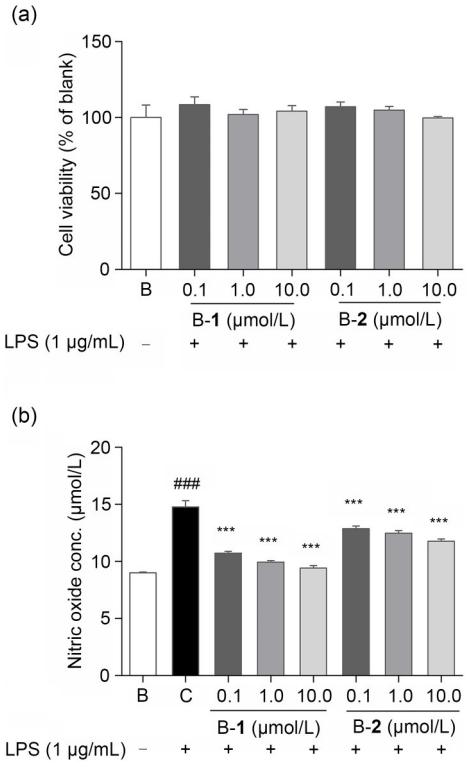

Fig. 3 Cell viability (a) and NO production (b) treated by benzaldehydes 1 and 2. Data were expressed as mean±SD (*n*=3). * *P*<0.001, vs. control; ### *P*<0.001, vs. blank. B: blank; C: control; B-1: benzaldehyde 1; B-2: benzaldehyde 2; NO: nitric oxide; LPS: lipopolysaccharide; conc.: concentration; SD: standard deviation.**

Western blotting was used to verify whether the two benzaldehydes had a remarkable impact on NO production by suppressing the activity of iNOS. As shown in Figs. 5a and 5b, the expression of iNOS in the blank group was 0.55, while it was 0.98 in the control group, significantly higher than that in the unstimulated state. However, NO production in the low-dose group (0.1 μmol/L) in the B-**1** and B-**2** groups was similar to the control group. Moreover, the expression of iNOS of the high-dose group (10.0 μmol/L) in the B-**1** and B-**2** groups was down-regulated and showed significant differences at a 95% confidence interval (CI). It is worth noting that, though it belongs to different doses of the groups, the expression of iNOS in the B-**1** group decreased more than that in the B-**2** group when applying the same dose.

Similar to iNOS, the expression of COX-2 presented a reduction trend after the pioneer experiment. The expression of COX-2 increased with a significant difference between the control group and the blank group. Moreover, the COX-2 level decreased in the B-**1** and B-**2** groups. Among them, the expression of COX-2 in the high-dose group (10.0 μmol/L) of the B-**1** and B-**2** groups decreased compared with the control group (Figs. 5a and 5c). The low-dose (0.1 μmol/L) of the B-**1** group was not as effective as the other sample groups, as it showed significant discrepancy.

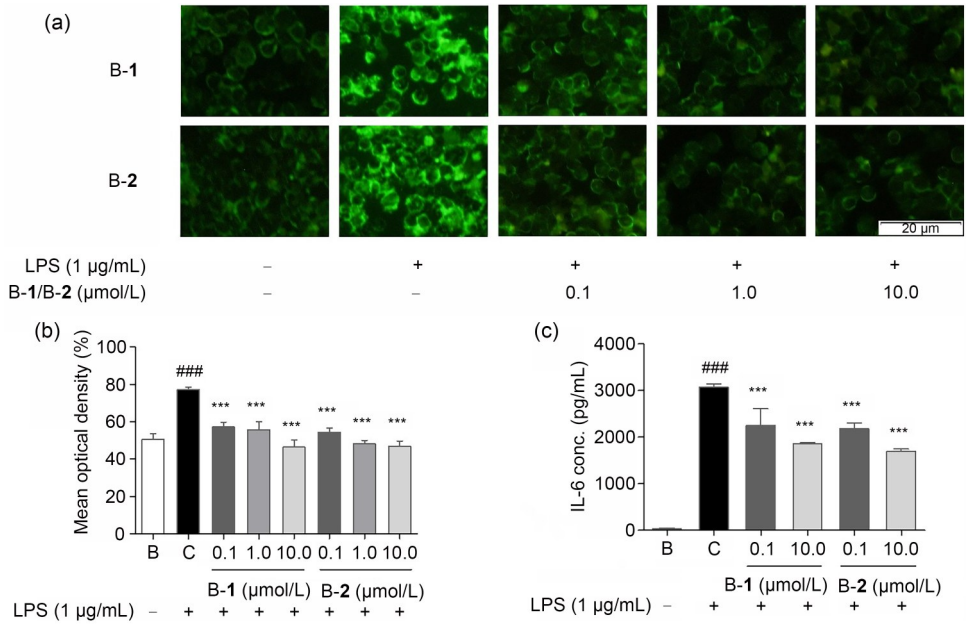

Fig. 4 ROS (a, b) and IL-6 (c) levels of cells treated by benzaldehydes 1 and 2. Data were expressed as mean±SD (*n*=3). * *P*<0.001, vs. control; ### *P*<0.001, vs. blank. B: blank; C: control; B-1: benzaldehyde 1; B-2: benzaldehyde 2; ROS: reactive oxygen species; IL-6: interleukin-6; LPS: lipopolysaccharide; SD: standard deviation; conc.: concentration.**

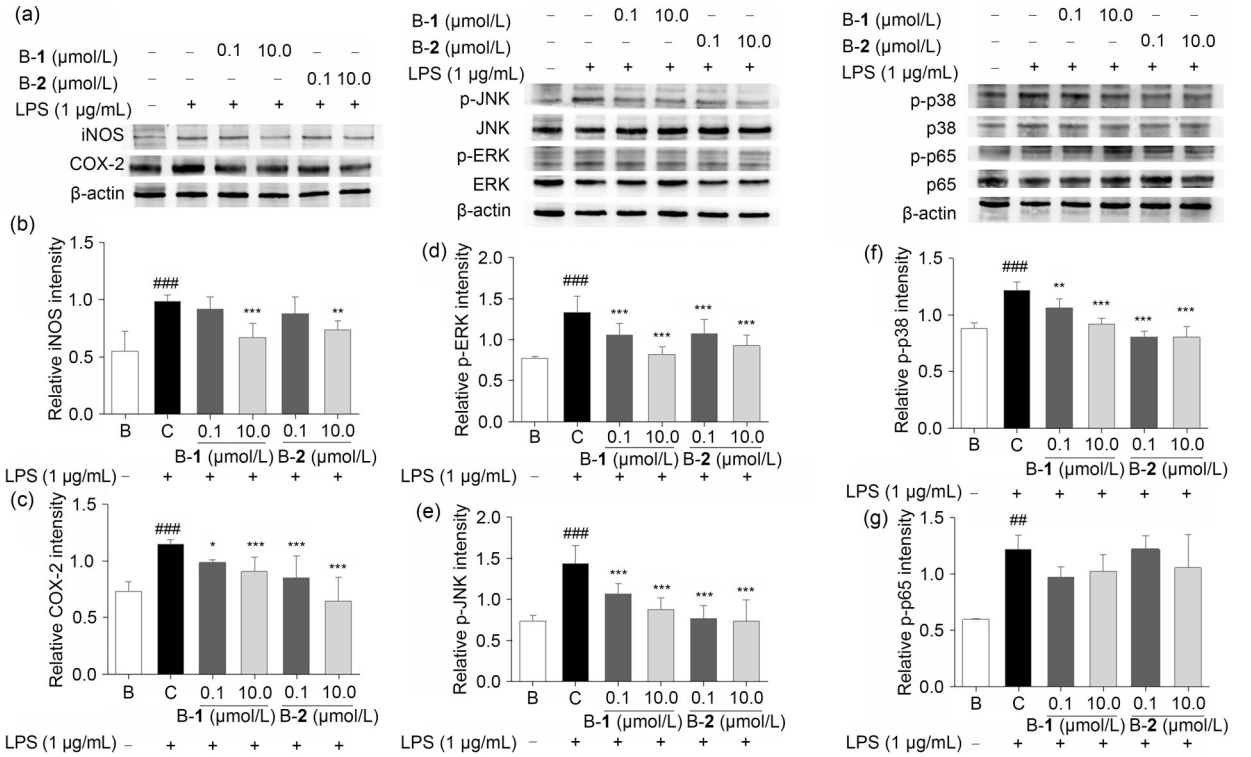

Fig. 5 Effects of two benzaldehydes on protein production in RAW264.7 cells. (a) Western blot analyses of iNOS, COX-2, p-ERK, ERK, p-JNK, JNK, p-p38, p38, p-p65, and p65, with β-actin as an internal control. iNOS (b), COX-2 (c), p-ERK (d), p-JNK (e), p-p38 (f), and p-p65 (g) productions of cells treated by benzaldehydes 1 and 2. Data were expressed as mean±SD (n=3). $^{\#\#}P$<0.01, $^{\#\#\#}P$<0.001, vs. blank; $^{*}P$<0.05, $^{**}P$<0.01, $^{***}P$<0.001, vs. control. iNOS: inducible nitric oxide synthase; COX-2: cyclooxygenase-2; ERK: extracellular signal-related kinase; JNK: c-Jun N-terminal kinase; p: phosphorylated; LPS: lipopolysaccharide; B: blank; C: control; B-1: benzaldehyde 1; B-2: benzaldehyde 2; SD: standard deviation.

Western blotting was conducted to identify whether the two benzaldehydes (**1** and **2**) played a role in anti-inflammation via restraining the expression of phosphorylated JNK (p-JNK), p-ERK, and p-p38 to block the transmission of signals of the MAPK signaling pathway.

As shown in Figs. 5a and 5d, the protein level of p-ERK exhibited a sharp increase in the control group. Also, the expression level of p-ERK had a monotone decreasing trend along with the increasing dose of the two benzaldehydes (**1** and **2**). Among them, there was a steeper slope in the B-**1** group than in the B-**2** group.

Similarly, p-JNK and p-p38 productions were elevated in the control group but declined in the B-**1** and B-**2** groups (Figs. 5a, 5e, and 5f). The variation tendency of the protein levels of p-JNK and p-p38 was different. The level of p-JNK decreased with the increasing dose of the two benzaldehydes (**1** and **2**), showing dose dependency. However, different from the B-**1** group, the expression of p-p38 slightly increased with the rising dose of benzaldehyde **2**. However, the two benzaldehydes (**1** and **2**) were still effective in down-regulating the expression levels of p-ERK, p-JNK, and p-p38, with significant differences when compared with the control groups.

This result demonstrated that the two benzaldehydes (**1** and **2**) could inhibit the activation of the MAPK signaling pathway in RAW264.7 cells.

Western blot assay was conducted to examine whether the two benzaldehydes (**1** and **2**) could restrain p-NF-κB p65 expression on the NF-κB signaling pathway. As shown in Figs. 5a and 5g, the protein level of p-NF-κB p65 increased in the control group when compared with the blank. In the B-**1** and B-**2** groups, the production of p-NF-κB p65 remained at a high level with no significant change compared with the control group. These results indicated that neither of the two benzaldehydes (**1** and **2**) could inhibit the phosphorylation of NF-κB-p65.

Molecular docking was performed to elucidate the interaction mode between COX-2 and the two benzaldehydes (**1** and **2**) at the molecular level. These two benzaldehydes (**1** and **2**) docked to the active pocket of COX-2 with an affinity of −7.5 and −7.7 kcal/mol, respectively. The theoretical binding mode was shown in Figs. 6a–6d. As shown in Figs. 6b and 6c, both of the two benzaldehydes (**1** and **2**) exhibited a compact binding pattern with the active pockets. Among the two, benzaldehyde **1** located in a cavity pocket consisted of amino acids Val335, Leu338, Ser339, Tyr341, Trp373, Phe504, Val509, Ala513, and Ser516, forming a strong hydrophobic interaction (Fig. 6a). Meanwhile, benzaldehyde **2** located in a cavity pocket consisted of amino acids Val335, Leu338, Ser339, Tyr371, Phe504, Met508, Val509, Gly512, Ala513, and Ser516, also forming a strong hydrophobic interaction (Fig. 6d). More importantly, benzaldehyde **1** formed 4.7 and 3.4 Å hydrogen bonds with amino acids Tyr341 and Phe504, respectively (Fig. 6a), and it formed π–π bonds with amino acid Ser339. Moreover, benzaldehyde **2** formed 3.9, 6.4, and 4.5 Å hydrogen bonds with amino acids Tyr371, Met508, and Ser516, respectively (Fig. 6d). These constituted the dominant force between the two benzaldehydes (**1** and **2**) and COX-2. All of these interactions allow both of the two benzaldehydes (**1** and **2**) to separately form a stable complex with COX-2.

In a similar fashion, as shown through the theoretical binding mode in Figs. 6e and 6h, benzaldehydes **1** and **2** were docked to the active pocket of iNOS with an affinity of −7.4 and −8.2 kcal/mol, respectively. As can be seen from Figs. 6f and 6g, both of the two benzaldehydes (**1** and **2**) exhibited a compact binding pattern in the active pocket. Benzaldehyde **1** was in a cavity pouch composed of amino acids Trp188, Cys194, Leu203, Ser236, Ile238, Pro344, Val346, Phe363, Asn364, Gly365, Trp366, and Tyr483, while benzaldehyde **2** was in a cavity pouch composed of amino acids Trp188, Ala191, Cys194, Leu203, Ser236, Ile238, Met349, Phe363, Asn364, Gly365, and Tyr483. A strong hydrophobic interaction was formed (Figs. 6e and 6h). Notably, benzaldehyde **1** could form 5.8 Å hydrogen bonds with amino acid Tyr483 (Fig. 6e) and π–π bonds with amino acids Trp188 and Phe363. Meanwhile, benzaldehyde **2** could form hydrogen bonds for 5.7 Å with the amino acid Tyr483 (Fig. 6h). These constituted the primary force between

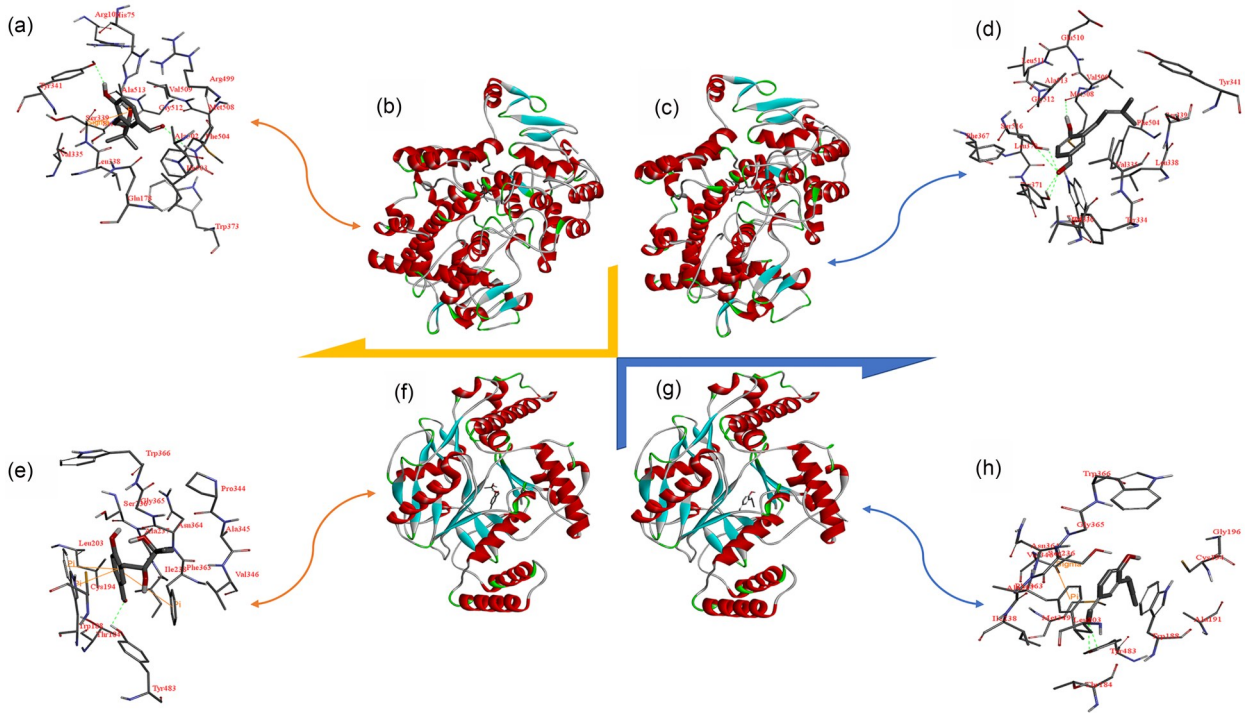

Fig. 6 Docking study of COX-2/iNOS with benzaldehydes 1 and 2. Docking study of COX-2 with benzaldehydes 1 (a, b) and 2 (c, d); Docking study of iNOS with benzaldehydes 1 (e, f) and 2 (g, h). iNOS: inducible nitric oxide synthase; COX-2: cyclooxygenase-2.

the benzaldehyde **1** and iNOS, similar to benzaldehyde **2** and iNOS. All of these interactions result in the formation of a stable complex of iNOS and benzaldehyde **1**, as well as benzaldehyde **2**. Given the above, we can conclude that the above molecular docking results provide a reasonable explanation for the interaction between benzaldehyde **1** and iNOS, as well as that between benzaldehyde **2** and iNOS, and lay the foundation for further studies of iNOS inhibitors.

In our previous studies (Yang et al., 2019, 2020), we evaluated the antioxidant capacity of the active components isolated from *A. terreus* C23-3 by thin-layer chromatography (TLC) bioautography. This analysis revealed that the extract has certain large polar antioxidant activity and strong acetylcholinesterase inhibition activity spots. Hence, further studies on the relevant inflammatory activity and mechanisms have been carried out.

Acute inflammation generally contributes to the restoration of tissue homeostasis, yet long-term uncontrolled acute inflammation may become chronic and lead to various long-term inflammatory diseases (Zhou et al., 2016). Inflammation involves a microcirculatory process with changes in vascular permeability, recruitment, and the accumulation of white blood cells, as well as the release of inflammatory mediators (Chertov et al., 2000; Ferrero-Miliani et al., 2007). The classical cell model for studying inflammation involves inhibiting the expression of iNOS and COX-2 in inflammatory cell lines, such as macrophage cell lines and microglia cell lines induced by LPS or interferon-γ (IFN-γ) (Cheung et al., 2016). In macrophages, stimuli like LPS are mainly from Gram-negative bacteria, which trigger downstream signaling, such as the activation of inhibitor of NF-κB kinase (IKK) proteins, further leading to activation of NF-κB and the up-regulation of a range of inflammatory genes. This finally results in the synthesis of inducible enzymes such as COX-2 and iNOS (Emam et al., 2021).

Earlier studies have implicated that a mass of iNOS is harmful and contributes to injury observed in many inflammatory models. In addition, iNOS can synthesize prodigious amounts of NO for certain periods (Laroux et al., 2001). Higher NO levels may in turn lead to inflammation, apoptosis, and oxidative stress (Nagy et al., 2007). It is noteworthy that ROS can result in neurotoxic damage through interacting with NO to produce more toxic intermediates (Cobourne-Duval et al., 2016). According to the results of molecular docking, our study discovered that benzaldehyde **1** can form hydrogen bonds with amino acid Tyr483 (Fig. 6e) and π–π bonds with amino acids Trp188 and Phe363, while benzaldehyde **2** can form hydrogen bonds with the amino acid Tyr483 (Fig. 6h). The evaluation of the results implies that both of the two benzaldehydes (**1** and **2**) can form a stable complex with iNOS. Nevertheless, because benzaldehyde **1** has more binding sites with iNOS than benzaldehyde **2**, it binds more firmly with iNOS. Accordingly, it can be speculated that benzaldehyde **1** has a better inhibition effect on iNOS and is more conducive to indirectly reducing the level of NO. Meanwhile, the results of western blot analysis implied that iNOS was obviously reduced in the B-**1** and B-**2** groups and decreased even more in the B-**1** group (Fig. 5b). On the other hand, although treated with different samples, the B-**1** and B-**2** groups shared a high degree of similarity in terms of low NO levels, and this level of the B-**1** group was lower than that of the B-**2** group. These results serve as additional evidence of the better inhibitory effect of benzaldehyde **1** on iNOS, and also it can more effectively reduce the concentration of NO. Hence, it can be assumed that the two benzaldehydes (**1** and **2**) can weaken inflammation by decreasing the expression of iNOS to further directly and indirectly decrease the level of NO. Meanwhile, COX-2 also plays an important role in the pathogenesis of inflammation. It is a kind of inducible enzyme that expresses rarely in normal tissues but much more under a series of intracellular and extracellular stimuli, such as LPS, tumor necrosis factor-α (TNF-α), and IL-1β (Wu et al., 2010; Xie et al., 2016). As the pivotal rate-limiting enzyme, COX-2 can catalyze the step in the formation of prostaglandin G_2 (PGG_2) from arachidonic acid. Subsequently, it further transforms into prostaglandin H_2 (PGH_2) that can induce inflammatory cells to release chemokines, recruit inflammatory cells to move, and cause the expression of IL-6 in macrophages in coordination with LPS (Oshima et al., 2011). Besides, ROS production in LPS-induced cells can give rise to inflammation by up-regulating the production of pro-inflammatory cytokines before acting as a second messenger in subsequent processes (Block et al., 2007). Cytokines like IL-6 regulate the immune response to infection or inflammation through a complex network of interactions and modulate

inflammation by themselves. However, the excessive production of inflammatory cytokines can lead to tissue damage, hemodynamic changes, organ failure, and ultimately death (Czaja, 2014; Liu et al., 2016). In the present study, we demonstrated that benzaldehyde **1** forms hydrogen bonds with amino acids Tyr341 and Phe504 (Fig. 6a) and π–π bonds with amino acid Ser339. Meanwhile, benzaldehyde **2** forms hydrogen bonds with amino acids Tyr371, Met508, and Ser516 (Fig. 6d). Thus, the two benzaldehydes (**1** and **2**) and COX-2 can form a stable complex. However, the hydrogen bond is stronger than the π–π bond, and the affinity between benzaldehyde **2** and COX-2 is −8.2 kcal/mol, which is stronger than that for benzaldehyde **1** (−7.4 kcal/mol). It can be presumed that benzaldehyde **2** has a better inhibitory effect on COX-2 than benzaldehyde **1**, and leads to a more indirect reduction in IL-6 levels. The results showed that less COX-2 was expressed in the B-**1** and B-**2** groups compared with the control group (Fig. 5c). Among them, the level of COX-2 in the B-**2** group was lower than that in the B-**1** group, which further confirmed that benzaldehydes (**1** and **2**) can effectively reduce the level of COX-2 and B-**2** has a better inhibitory effect. Additionally, COX-2 and ROS can indirectly induce IL-6 expression in macrophages. As shown in Figs. 4b and 4c, the ROS and IL-6 levels in the B-**1** and B-**2** groups were generally lower than those in the control group, demonstrating that the two benzaldehydes (**1** and **2**) were capable of reducing ROS and IL-6 levels and relieving the level of oxidative stress. Among them, B-**2** has a slightly better effect. Combining the above molecular docking studies provides a reasonable explanation for the interaction between the two benzaldehydes (**1** and **2**) and the two inflammatory factors (COX-2 and iNOS).

ROS, as one of the significant molecular targets of inflammatory diseases, can activate multiple signaling pathways, among which the NF-κB and MAPK signaling pathways are closely related to inflammation regulation (Li et al., 2009). However, the two benzaldehydes (**1** and **2**) did not inhibit the expression of p-p65 in our study. The MAPK signaling pathways play an important role in inflammation. The common feature of MAPK signaling pathways is that MAPK kinase kinase (MAPKKK), a serine/threonine-protein kinase, is activated and phosphorylated to activate MAPK kinase (MAPKK), which is further phosphorylated to activate MAPK. After different kinds of extracellular chemical signals are combined with corresponding cell membrane receptors, different MAPKs can be activated through different MAPK cascade signal-transducing pathways to mediate separate cellular biological reactions (Arbabi and Maier, 2002). MAPKs, including extracellular signal-regulated kinase ERK1/2, p38 MAPK, and JNKs, belong to a family of serine/threonine protein kinases, which can transfer the information perceived from extracellular stimuli to the cell (Kim and Choi, 2010). Among them, ERKs are usually activated by mitogen and differentiation signaling, while JNK and p38 are activated by inflammatory stimuli and stress (Sabio and Davis, 2014). In general, the activation of ERK1/2 and JNK can also lead to the phosphorylation and activation of p38 transcription factors in the cytoplasm or nucleus, thereby triggering inflammatory responses (Raingeaud et al., 1996; Chen et al., 2018). In addition, the phosphorylation of MAPK activates the NF-κB signaling pathway and promotes the expression of iNOS (Martínez-Soto and Ruiz-Herrera, 2017). Our results indicate that the expression of p-ERK, p-JNK, and p-p38 exhibited a distinct decrease after treatment with either of the two benzaldehydes (**1** and **2**) in the LPS-induced cell. Consequently, both of the two benzaldehydes (**1** and **2**) have an anti-inflammatory effect by selectively inhibiting the levels of p-ERK, p-JNK, and p-p38 in the MAPK signaling pathway in macrophage cells.

The derivatives of benzaldehyde from *Aspergillus* sp. of marine origin were isolated in a previous study. An et al. (2019) isolated thirteen compounds from the secondary metabolites of marine fungus *Aspergillus* sp. SCS-KFD66. Among them, aloe-emodin, citreorosein, protocatechualdehyde, 2,5-dihydroxybenzaldehyde, and 4-hydroxybenzoic acid can be derived from benzaldehyde. Also, two compounds (**1** and **2**) are derived from benzaldehyde. Benzaldehyde **1** is the new compound in our study, whose structure is similar to benzaldehyde **2**, and they were isolated from secondary metabolites. It could be hypothesized that benzaldehyde **1** was transferred from benzaldehyde **2** (Fig. 7). There was a large amount of water in the fermentation broth, so it can be assumed that benzaldehyde **2** possibly reacted with H_2O. Furthermore, the inflammatory effect was determined by measuring the productions of NO, ROS, IL-6, iNOS, COX-2, p-ERK, p-JNK, p-p38, and p-p65. The results showed that the

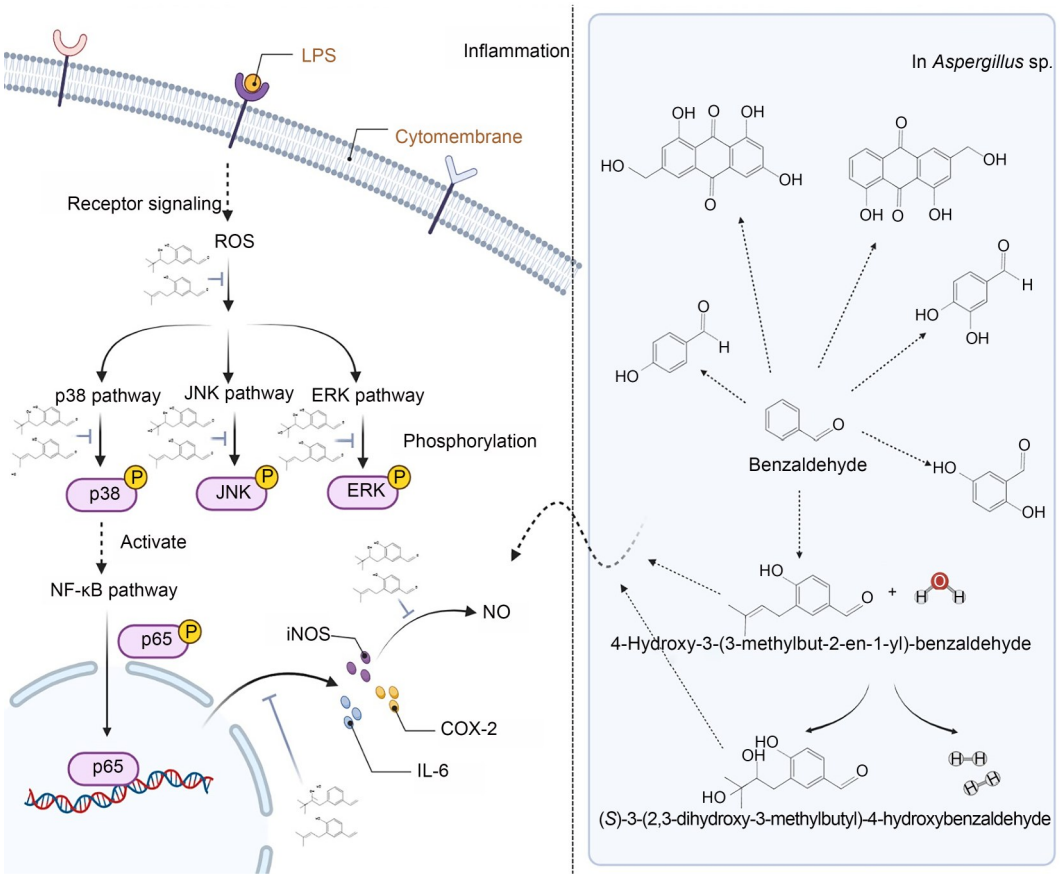

Fig. 7 Benzaldehyde and its derivatives and a schematic diagram, which illustrates the feasible signaling mechanisms of benzaldehydes 1 and 2 to reduce the LPS-induced inflammation in cells. Benzaldehydes 1 and 2 could inhibit the release of NO and ROS, and block the protein expression of IL-6, iNOS and COX-2 and phosphorylation levels of ERK, JNK and p38. LPS: lipopolysaccharide; ROS: reactive oxygen species; JNK: c-Jun N-terminal kinase; ERK: extracellular signal-related kinase; NF-κB: nuclear factor-κB; iNOS: inducible nitric oxide synthase; COX-2: cyclooxygenase-2; NO: nitric oxide; IL-6: interleukin-6.

two benzaldehydes (**1** and **2**) could reduce inflammation to a certain degree.

In summary, this paper reported that two benzaldehydes (**1** and **2**) have been isolated from a coral-derived *A. terreus* strain C23-3. After a series of structural identification, it could be ascertained that one of them was 4-hydroxy-3-(3-methylbut-2-en-1-yl)-benzaldehyde, and the other is a new benzaldehyde ((*S*)-3-(2,3-dihydroxy-3-methylbutyl)-4-hydroxybenzaldehyde). The findings reported here have revealed that both of the two benzaldehydes (**1** and **2**) could reduce the levels of some inflammatory biomarkers. Moreover, in all doses, both could significantly inhibit the release of NO and ROS, and effectively block the protein expression of IL-6, iNOS and COX-2 and phosphorylation levels of ERK, JNK and p38. Overall, these two benzaldehydes may have potential applications in inflammation-related diseases in the future.

Materials and methods

Detailed methods are provided in the electronic supplementary materials of this paper.

Acknowledgments

This work was supported by the Natural Science Foundation of Guangdong Province (No. 2018A030307046), the Basic Research Project of Shenzhen Science and Technology Innovation Commission (No. JCYJ20190813105005619), the Shenzhen Dapeng New District Industrial Development Fund (No. KY20180203), the Shenzhen Dapeng New District Scientific and Technological Research and Development Fund (No. KJYF202001-07), and the the Innovation and Development Project about Marine Economy Demostration of Zhanjiang City (No. XM-202008-01B1), China.

Author contributions

Minqi CHEN performed the experimental research and data analysis, wrote and edited the manuscript. Jinyue LIANG, Yuan WANG, Yayue LIU, Chunxia ZHOU, and Pengzhi HONG performed the experimental research. Zhong-Ji QIAN and Yi ZHANG contributed to the study design. All authors have read and approved the final manuscript, and therefore, have full access to all the data in the study and take responsibility for the integrity and security of the data.

Compliance with ethics guidelines

Minqi CHEN, Jinyue LIANG, Yuan WANG, Yayue LIU, Chunxia ZHOU, Pengzhi HONG, Yi ZHANG, and Zhong-Ji QIAN declare that they have no conflict of interest.

This article does not contain any studies with human or animal subjects performed by any of the authors.

References

Afonina IS, Zhong ZY, Karin M, et al., 2017. Limiting inflammation—the negative regulation of NF-κB and the NLRP3 inflammasome. *Nat Immunol*, 18(8):861-869. https://doi.org/10.1038/ni.3772

Aktan F, 2004. iNOS-mediated nitric oxide production and its regulation. *Life Sci*, 75(6):639-653. https://doi.org/10.1016/j.lfs.2003.10.042

An CL, Kong FD, Ma QY, et al., 2019. Secondary metabolites from marine-derived fungus *Aspergillus* sp. SCS-KFD66. *Chin Tradit Herb Drugs*, 50(13):3001-3007 (in Chinese). https://doi.org/10.7501/j.issn.0253-2670.2019.13.002

Arbabi S, Maier RV, 2002. Mitogen-activated protein kinases. *Crit Care Med*, 30(1):S74-S79. https://doi.org/10.1097/00003246-200201001-00010

Block ML, Zecca L, Hong JS, 2007. Microglia-mediated neurotoxicity: uncovering the molecular mechanisms. *Nat Rev Neurosci*, 8(1):57-69. https://doi.org/10.1038/nrn2038

Chen LL, Deng HD, Cui HM, et al., 2018. Inflammatory responses and inflammation-associated diseases in organs. *Oncotarget*, 9(6):7204-7218. https://doi.org/10.18632/oncotarget.23208

Chen N, Yu SK, Liu B, et al., 2019. Advances in research on secondary metabolites and activities of marine fungi. *Chin J Public Health Manag*, 35(1):44-47 (in Chinese). https://doi.org/10.19568/j.cnki.23-1318.2019.01.012

Chertov O, Yang D, Howard OMZ, et al., 2000. Leukocyte granule proteins mobilize innate host defenses and adaptive immune responses. *Immunol Rev*, 177(1):68-78. https://doi.org/10.1034/j.1600-065X.2000.17702.x

Cheung RCF, Ng TB, Wong JH, et al., 2016. Marine natural products with anti-inflammatory activity. *Appl Microbiol Biotechnol*, 100(4):1645-1666. https://doi.org/10.1007/s00253-015-7244-3

Cho JY, Kim MS, 2012. Antibacterial benzaldehydes produced by seaweed-derived *Streptomyces atrovirens* PK288-21. *Fish Sci*, 78(5):1065-1073. https://doi.org/10.1007/s12562-012-0531-3

Cobourne-Duval MK, Taka E, Mendonca P, et al., 2016. The antioxidant effects of thymoquinone in activated BV-2 murine microglial cells. *Neurochem Res*, 41(12):3227-3238. https://doi.org/10.1007/s11064-016-2047-1

Czaja AJ, 2014. Hepatic inflammation and progressive liver fibrosis in chronic liver disease. *World J Gastroenterol*, 20(10):2515-2532. https://doi.org/10.3748/wjg.v20.i10.2515

Emam SH, Sonousi A, Osman EO, et al., 2021. Design and synthesis of methoxyphenyl- and coumarin-based chalcone derivatives as anti-inflammatory agents by inhibition of NO production and down-regulation of NF-κB in LPS-induced RAW264.7 macrophage cells. *Bioorg Chem*, 107: 104630. https://doi.org/10.1016/j.bioorg.2021.104630

Ferrero-Miliani L, Nielsen OH, Andersen PS, et al., 2007. Chronic inflammation: importance of NOD2 and NALP3 in interleukin-1β generation. *Clin Exp Immunol*, 147(2): 227-235. https://doi.org/10.1111/j.1365-2249.2006.03261.x

Hayden MS, Ghosh S, 2008. Shared principles in NF-κB signaling. *Cell*, 132(3):344-362. https://doi.org/10.1016/j.*cell*.2008.01.020

Kim EK, Choi EJ, 2010. Pathological roles of MAPK signaling pathways in human diseases. *Biochim Biophys Acta*, 1802(4):396-405. https://doi.org/10.1016/j.bbadis.2009.12.009

Kim KS, Cui X, Lee DS, et al., 2014. Inhibitory effects of benzaldehyde derivatives from the marine fungus *Eurotium* sp. SF-5989 on inflammatory mediators via the induction of heme oxygenase-1 in lipopolysaccharide-stimulated RAW264.7 macrophages. *Int J Mol Sci*, 15(12):23749-23765. https://doi.org/10.3390/ijms151223749

Kröncke KD, Fehsel K, Kolb-Bachofen V, 1998. Inducible nitric oxide synthase in human diseases. *Clin Exp Immunol*, 113(2):147-156. https://doi.org/10.1046/j.1365-2249.1998.00648.x

Laroux FS, Pavlick KP, Hines IN, et al., 2001. Role of nitric oxide in inflammation. *Acta Physiol Scand*, 173(1):113-118. https://doi.org/10.1046/j.1365-201X.2001.00891.x

Lawrence T, Willoughby DA, Gilroy DW, 2002. Anti-inflammatory lipid mediators and insights into the resolution of inflammation. *Nat Rev Immunol*, 2(10):787-795. https://doi.org/10.1038/nri915

Li L, Wang LY, Wu ZQ, et al., 2014. Anthocyanin-rich fractions from red raspberries attenuate inflammation in both RAW264.7 macrophages and a mouse model of colitis. *Sci Rep*, 4:6234. https://doi.org/10.1038/srep06234

Li ST, Dai Q, Zhang SX, et al., 2018. Ulinastatin attenuates LPS-induced inflammation in mouse macrophage RAW264.7 cells by inhibiting the JNK/NF-κB signaling pathway and activating the PI3K/Akt/Nrf2 pathway. *Acta Pharmacol Sin*, 39(8):1294-1304. https://doi.org/10.1038/aps.2017.143

Li Z, Chen-Roetling J, Regan RF, 2009. Increasing expression of H- or L-ferritin protects cortical astrocytes from hemin

toxicity. *Free Radic Res*, 43(6):613-621. https://doi.org/10.1080/10715760902942808

Liu ZG, Wang YP, Wang YQ, et al., 2016. Dexmedetomidine attenuates inflammatory reaction in the lung tissues of septic mice by activating cholinergic anti-inflammatory pathway. *Int Immunopharmacol*, 35:210-216. https://doi.org/10.1016/j.intimp.2016.04.003

Ma XX, Liu YY, Nie YY, et al., 2021. LC-MS/MS based molecular network analysis of the effects of chemical regulation on the secondary metabolites and biological activities of a fungal strain *Aspergillus terreus* C23-3. *Biotechnol Bull*, 37(8):95-110 (in Chinese). https://doi.org/10.13560/j.cnki.biotech.bull.1985.2020-1398

Machado FP, Kumla D, Pereira JA, et al., 2021. Prenylated phenylbutyrolactones from cultures of a marine sponge-associated fungus *Aspergillus flavipes* KUFA1152. *Phytochemistry*, 185:112709. https://doi.org/10.1016/j.phytochem.2021.112709

Marletta MA, 1993. Nitric oxide synthase structure and mechanism. *J Biol Chem*, 268(17):12231-12234. https://doi.org/10.1016/S0021-9258(18)31375-9

Martínez-Soto D, Ruiz-Herrera J, 2017. Functional analysis of the MAPK pathways in fungi. *Rev Iberoam Micol*, 34(4):192-202. https://doi.org/10.1016/j.riam.2017.02.006

Moncada S, Higgs EA, 1991. Endogenous nitric oxide: physiology, pathology and clinical relevance. *Eur J Clin Invest*, 21(4):361-374. https://doi.org/10.1111/j.1365-2362.1991.tb01383.x

Nagy G, Clark JM, Buzás EI, et al., 2007. Nitric oxide, chronic inflammation and autoimmunity. *Immunol Lett*, 111(1):1-5. https://doi.org/10.1016/j.imlet.2007.04.013

Nie YY, Yang WC, Liu YY, et al., 2020. Acetylcholinesterase inhibitors and antioxidants mining from marine fungi: bioassays, bioactivity coupled LC-MS/MS analyses and molecular networking. *Mar Life Sci Technol*, 2(4):386-397. https://doi.org/10.1007/s42995-020-00065-9

Oshima H, Hioki K, Popivanova BK, et al., 2011. Prostaglandin E_2 signaling and bacterial infection recruit tumor-promoting macrophages to mouse gastric tumors. *Gastroenterology*, 140(2):596-607.E7. https://doi.org/10.1053/j.gastro.2010.11.007

Pinho-Ribeiro FA, Zarpelon AC, Mizokami SS, et al., 2016. The citrus flavonone naringenin reduces lipopolysaccharide-induced inflammatory pain and leukocyte recruitment by inhibiting NF-κB activation. *J Nutr Biochem*, 33:8-14. https://doi.org/10.1016/j.jnutbio.2016.03.013

Raingeaud J, Whitmarsh AJ, Barrett T, et al., 1996. MKK3- and MKK6-regulated gene expression is mediated by the p38 mitogen-activated protein kinase signal transduction pathway. *Mol Cell Biol*, 16(3):1247-1255. https://doi.org/10.1128/MCB.16.3.1247

Sabio G, Davis RJ, 2014. TNF and MAP kinase signalling pathways. *Semin Immunol*, 26(3):237-245. https://doi.org/10.1016/j.smim.2014.02.009

Umeda M, Yamashita T, Saito M, et al., 1974. Chemical and cytotoxicity survey on the metabolites of toxic fungi. *Jpn J Exp Med*, 44(1):83-96.

Wang S, Li XM, Teuscher F, et al., 2006. Chaetopyranin, a benzaldehyde derivative, and other related metabolites from *Chaetomium globosum*, an endophytic fungus derived from the marine red alga *Polysiphonia urceolata*. *J Nat Prod*, 69(11):1622-1625. https://doi.org/10.1021/np060248n

Wu CY, Chi PL, Hsieh HL, et al., 2010. TLR4-dependent induction of vascular adhesion molecule-1 in rheumatoid arthritis synovial fibroblasts: roles of cytosolic phospholipase $A_2\alpha$/cyclooxygenase-2. *J Cell Physiol*, 223(2):480-491. https://doi.org/10.1002/jcp.22059

Xie X, Ying WY, Jin SW, 2016. Research progress of cyclooxygenase-2 in the resolution of inflammation. *Chem Life*, 36(4):461-464 (in Chinese). https://doi.org/10.13488/j.smhx.20160406

Xin Y, Yuan Q, Liu CQ, et al., 2020. MiR-155/GSK-3β mediates anti-inflammatory effect of Chikusetsusaponin IVa by inhibiting NF-κB signaling pathway in LPS-induced RAW264.7 cell. *Sci Rep*, 10:18303. https://doi.org/10.1038/s41598-020-75358-1

Yamanishi R, Yoshigai E, Okuyama T, et al., 2014. The anti-inflammatory effects of flavanol-rich lychee fruit extract in rat hepatocytes. *PLoS ONE*, 9(4):e93818. https://doi.org/10.1371/journal.pone.0093818

Yang JM, Yang WC, Liu YY, et al., 2019. Influence of chemical induction on the secondary metabolites and biological activities of a marine-derived fungal strain *Aspergillus terreus* C23-3. *Microbiol China*, 46(3):441-452 (in Chinese). https://doi.org/10.13344/j.microbiol.china.180651

Yang JM, Liu YY, Yang WC, et al., 2020. An anti-inflammatory isoflavone from soybean inoculated with a marine fungus *Aspergillus terreus* C23-3. *Biosci Biotechnol Biochem*, 84(8):1546-1553. https://doi.org/10.1080/09168451.2020.1764838

Zhao MB, Zhou SX, Zhang QY, et al., 2017. Prenylated benzoic acid derivatives from the stem of *Euodia lepta*. *Nat Prod Res*, 31(13):1589-1593. https://doi.org/10.1080/14786419.2017.1283493

Zhou Y, Hong Y, Huang HH, 2016. Triptolide attenuates inflammatory response in membranous glomerulonephritis rat via downregulation of NF-κB signaling pathway. *Kidney Blood Press Res*, 41(6):901-910. https://doi.org/10.1159/000452591

Zucoloto AZ, Manchope MF, Staurengo-Ferrari L, et al., 2017. Probucol attenuates lipopolysaccharide-induced leukocyte recruitment and inflammatory hyperalgesia: effect on NF-κB activation and cytokine production. *Eur J Pharmacol*, 809:52-63. https://doi.org/10.1016/j.ejphar.2017.05.016

Supplementary information

Materials and methods; Figs. S1–S7